UNDERSTANDING THE SPACE WEATHERING OF MERCURY VIA SIMULATION OF MICROMETEORITE IMPACTS. M. L. McGlaun[1], M. S. Thompson[1], K. E. Vander Kaaden[2], M. J. Loeffler[3], F. M. McCubbin[4], Z. Rahman[2], and P. Haenecour[5]. [1]Department of Earth, Atmospheric, and Planetary Sciences, Purdue University, West Lafayette, IN, 47907, (mmcglaun@purdue.edu) [2]Jacobs, NASA Johnson Space Center, Houston, TX, 77058, [3]Northern Arizona University, Flagstaff, AZ, 86011, [4]ARES, NASA Johnson Space Center, Houston, TX, 77058, [5]Lunar and Planetary Laboratory, University of Arizona, Tucson, AZ, 85721.

Introduction: Space weathering alters the surfaces of airless planetary bodies via irradiation from the solar wind and micrometeorite impacts [1,2]. These processes modify the microstructure, chemical composition, and spectral properties of surface materials, typically resulting in the reddening (increasing reflectance with increasing wavelength), darkening (reducing albedo), and attenuation of characteristic absorption features in reflectance spectra [2,3]. In lunar samples, these changes in optical properties are driven by the production of reduced nanophase Fe particles (npFe). Our understanding of space weathering has largely been based on data from the Moon and, more recently, near-Earth S-type asteroids. However, the environment at Mercury is significantly different, with the surface experiencing intense solar wind irradiation and higher velocity micrometeorite impacts [4]. Additionally, the composition of Mercury's surface varies significantly from that of the Moon, including a component with very low albedo known as low reflectance material (LRM) which is enriched with up to 4 wt.% carbon over the local mean [5]. Our understanding of how carbon phases, including graphite, are altered as a result of these processes is limited [6].

In order to understand how space weathering affects the chemical, microstructural, and optical properties of the surface of Mercury, we can simulate these processes in the laboratory [6]. Here we use pulsed laser irradiation of sample mixtures of olivine and graphite to simulate micrometeorite impacts of the Mercurian surface. Pulsed laser irradiation simulates the short duration, high-temperature events associated with micrometeorite impacts on airless surfaces [7]. We then perform reflectance spectroscopy and electron microscopy to investigate the spectral, chemical, and microstructural changes in these samples.

Methods: We prepared a pressed powder pellet sample composed of San Carlos olivine (to maintain a pellet structure), with a surface layer of olivine mixed plus 5 wt.% powdered graphite. The grain sizes ranged from 45 to 125 μm. Samples were irradiated at Northern Arizona University, rastering a pulsed Nd-YAG laser beam, (λ=1064 nm, ~6 ns pulse duration, energy of 48 mJ/pulse) over the sample while under vacuum. The laser was rastered 1x and then 5x over the surface of the sample. We collected an situ reflectance spectrum from the surface of the sample after each laser pulse, using a Nicolet IS50 FTIR spectrometer with a wavelength range of 0.65-2.5 μm. We placed a silicon wafer near the surface of the sample in order to capture the melt and/or vapor deposits which were produced during the laser irradiation and ejected from the sample surface. We used the FEI Quanta 3D focused ion beam scanning electron microscope (FIB-SEM) at Johnson Space Center to extract sections from the surfaces of both the pressed pellet and the Si wafer. To image and chemically map the samples we used the Hitachi SU9000 30 keV scanning and transmission electron microscope (STEM/SEM) at the University of Arizona equipped with secondary electron, bright-field and dark-field detectors and an Oxford X-Max 100TLE energy-dispersive X-ray spectrometer (EDS).

Results: Coordinated analyses reveal complex microstructural and spectral effects.

Reflectance Spectroscopy: The brightness (absolute reflectance) of the surface increases after the 1x laser irradiation (Fig. 1). In addition, we observe a deeper 1.0 μm absorption feature for the 1x lasered sample compared to the unirradiated surface. In contrast, we observe that the brightness of the sample decreased to its lowest absolute reflectance after the 5x laser irradiation. Similarly, the depth of the 1.0 μm absorption features decreases to its lowest value for the 5x lasered sample.

Chemical and Microstructural Analysis: We observe multiple changes in the microstructural and chemical composition of the pressed powder samples. Analysis of the surface of the FIB section extracted from the

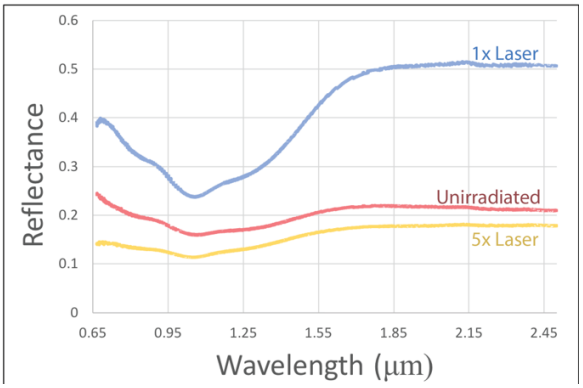

Figure 1: Reflectance data for the unirradiated, 1x, and 5x lasered samples. Note the initial brightening and subsequent darkening of the material with continued laser irradiation.

pellet reveal the presence of rounded C deposits measuring ~1 μm in diameter (Fig. 2a), with adjacent small olivine grains. This C-globule was likely produced via melting from the laser. This observed microstructure is considerably different from the graphite we observe at depth in the sample, comprised of discretely stacked

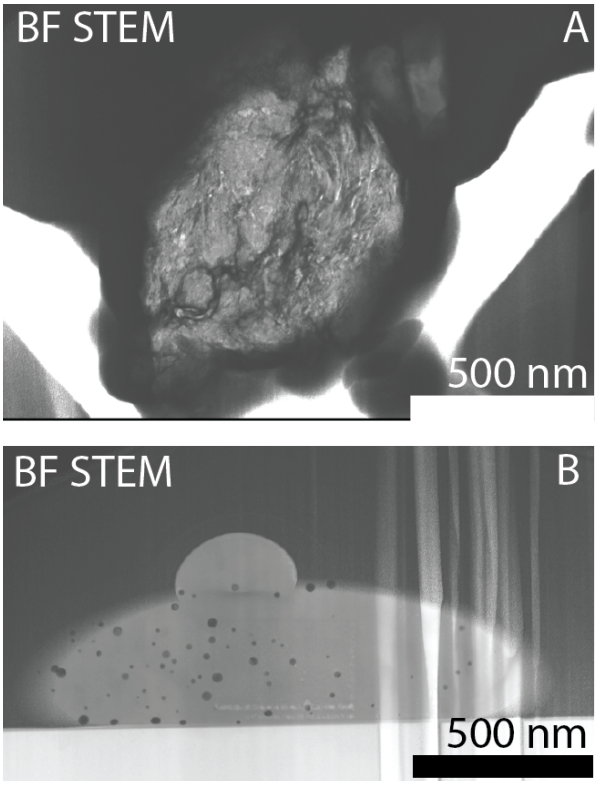

Figure 2: TEM data for FIB sections extracted from A) the pressed pellet showing melted carbon globule, and B) the Si wafer showing the compound melt deposit with Fe nanoparticles.

layers, and which appear unaltered by the laser.

The FIB section extracted from the Si wafer reveals the presence of multiple amorphous deposits distributed across the surface. These features have a distinct, pancake-like morphology (flat-top, rounded edges) which suggests they were melt droplets that impacted the surface of the Si wafer after ejection from the surface of the pellet during laser irradiation. One of these deposits has a compound morphology, with a small melt spherule superimposed on the surface of an underlying pancake-shaped layer. The indentation of the droplet suggests it impacted the surface after the initial deposit had cooled. This relationship indicates these deposits may have formed in separate irradiation events.

EDS chemical maps of these melt features indicate they are composed of Fe, Mg, Si and O. Regions of the compound deposit contains isolated Fe nanoparticles measuring up to ~25 nm in diameter (Fig. 3).

Implications for Space Weathering of Mercury: The spectral results observed here are inconsistent with previous experiments simulating the space weathering of Mercury [6,8]. In previous experiments, laser irradiation of pure olivine and pyroxene, and of quartz mixed with 5 wt.% graphite all resulted in the darkening and reddening of the reflectance spectra [6,8]. However, the exclusion of graphite and/or Fe-bearing phases from these experiments may not be entirely representative of the Mercurian surface. In our samples, the graphite functions as the darkening agent for the spectra. The initial laser raster may have functioned to preferentially melt and/or vaporize the (volatile) graphite phases, the results of which may be represented by the C-globule on the surface of the sample. These processes may result in the preferential removal of C-species from the surface of the sample, or may have caused the amalgamation of discrete C-bearing phases into larger, globule-style deposits. Both of these processes may have resulted in the initial brightening of the sample and may be indicative of the morphologies we expect for C-bearing species in the LRM on the surface of Mercury.

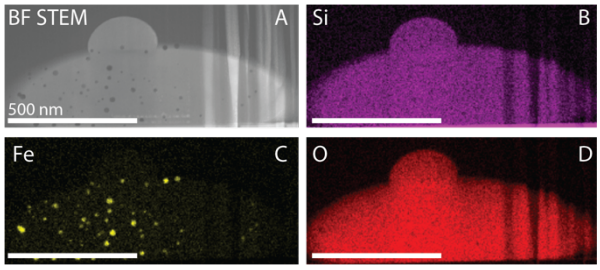

Figure 3: TEM data for the deposit shown in A) BF STEM image and EDS maps of B) Si, C) Fe, and D) O.

After the 1x laser raster, the removal and/or combination of graphite particles may have exposed more Fe-bearing olivine to the laser, resulting in the production of Fe nanoparticle-bearing melt/vapor deposits that we observe on the surface of the Si wafer. The production of these nanoparticles may have resulted in the observed eventual darkening and reduction of absorption bands in the 5x lasered sample. Further work is needed to explore the dependence of these spectral and chemical changes as a result of e.g., exposure timescale, Fe content, and grain size.

References: [1] Hapke B. (2001) *J. Geophys. Res.-Planet., 106,* 10039–10073. [2] Pieters C.M. and Noble S.K. (2016) *J. Geophys. Res-Planet., 121,* 1865–1884. [3] Keller L.P. et al. (1998) *LPS XXIX,* Abstract 1762. [4] Cintala M.J. (1992) *J. Geophys. Res.-Planet., 97,* 947–973. [5] Klima, R.L. et al. (2018) *Geophys. Res. Letters*, *45*, 2945–2953. [6] Trang D. et al. (2018) *LPS XLIX,* Abstract # 2083. [7] Sasaki, S. et al. (2001) *Nature, 410,* 555–557. [8] Sasaki, S. and Kurahashi, E. (2004) Space weathering on Mercury, *Adv. Space Res.*, 33, 2152-2155.